ELSEVIER

27 May 1994

Chemical Physics Letters 222 (1994) 471–480

CHEMICAL PHYSICS LETTERS

Kinetic energy effects on product state distributions in the $C(^3P)+N_2O(\tilde{X}\,^1\Sigma^+)$ reaction. Energy partitioning between the $NO(X\,^2\Pi)$ and $CN(X\,^2\Sigma^+)$ products

D.C. Scott [1], F. Winterbottom [2], M.R. Scholefield, S. Goyal, H. Reisler

Department of Chemistry, University of Southern California, Los Angeles, CA 90089-0482, USA

Received 17 February 1994; in final form 24 March 1994

Abstract

The reaction $C(^3P)+N_2O(\tilde{X}\,^1\Sigma^+)$ is studied by varying the kinetic energy of $C(^3P)$ in two center-of-mass regimes: 0.1–0.2 eV and 2–7 eV. $C(^3P)$ is directly observed, and the C_n velocity distribution is estimated from the time-of-flight of C_2. $CN(X\,^2\Sigma^+)$ is vibrationally inverted and rotationally 'hot' at all collision energies. $NO(X\,^2\Pi)$ is vibrationally much colder, but rotationally 'hot' at the higher collision energies. At lower energies, $NO(X\,^2\Pi)$ has no vibrational excitation and is cold rotationally. Thus, little energy flow occurs between the 'old' NO and 'new' CN bond, suggesting a predominantly direct reaction mechanism.

1. Introduction

Valuable insights into the reaction dynamics of atom–molecule reactions can be gained from studies carried out under well specified initial conditions, and with quantum state-resolved product detection. Specifically, the vibrational and rotational (v, R) state distributions of both products can reveal important mechanistic details. Recently, we studied the reaction $C(^3P)+N_2O$ at high collision energies and reported the $CN(X\,^2\Sigma^+)$ and $NO(X\,^2\Pi)$ product state distributions [1]. For this reaction, the symmetry correlation and spin conservation rules for an intermediate of C_s symmetry allow the reaction of ground state atomic carbon with nitrous oxide to occur through the following channels:

$$C(^3P_J)+N_2O(\tilde{X}\,^1\Sigma^+)\rightarrow CO(a\,^3\Pi)+N_2(X\,^1\Sigma^+),\quad \Delta H=-3.41\ \text{eV}, \tag{1}$$

$$C(^3P_J)+N_2O(\tilde{X}\,^1\Sigma^+)\rightarrow CO(X\,^1\Sigma^+)+N_2(B\,^3\Pi),\quad \Delta H=-2.07\ \text{eV}, \tag{2}$$

$$C(^3P_J)+N_2O(\tilde{X}\,^1\Sigma^+)\rightarrow CN(X\,^2\Sigma^+)+NO(X\,^2\Pi),\quad \Delta H=-2.88\ \text{eV}, \tag{3}$$

$$C(^3P_J)+N_2O(\tilde{X}\,^1\Sigma^+)\rightarrow CN(A\,^2\Pi)+NO(X\,^2\Pi),\quad \Delta H=-1.47\ \text{eV}. \tag{4}$$

The focus of our work has been the investigation of reaction products from channel (3) using laser-induced fluorescence (LIF). For the other channels, chemiluminescence from the electronically excited

[1] Present address: Jet Propulsion Laboratory, MS 183-401, Pasadena, CA 91109-8099, USA.

[2] Present address: Physical Chemistry Laboratory, Oxford University, South Parks Road, Oxford OX1 3QZ, UK.

Elsevier Science B.V.
SSDI 0009-2614(94)00380-9

products of reactions (1) and (2) has not been observed. CN(A→X) chemiluminescence from reaction (4) has been observed by Costes et al. in one study [2], but was not detected by Sekiya et al. [3] In addition, some theoretical work has also been reported [4,5].

In the past, the reactions of atomic carbon have been difficult to study in molecular beams due to the refractory nature of the element. An efficient method for production of ground state atomic carbon, $C(^3P)$, is laser ablation of graphite [6,7]. Laser ablation has proven to be a much cleaner source of atomic carbon compared to photolytic [8] or effusive sources [9].

In this Letter, we report changes in the energy disposal into the NO product while varying the translational energy of the carbon beam. The results were obtained by using two separate methods for production of atomic carbon: (i) free laser ablation of graphite and (ii) seeding the ablated carbon in various carrier gases through a pulsed supersonic valve [10]. Collisional energies in the range of 4.5 ± 2.5 eV can be obtained for the first method, while by seeding in He in the second method, energies in the range of 0.1–0.2 eV are obtained. In these studies, a vibrational population inversion was consistently observed for the $CN(X\,^2\Sigma^+)$ product with peak population around $v=3$ and bandheads up to $v=7$ identifiable at all collision energies. Also, significant rotational excitation was observed [1,11,12]. In contrast, the $NO(X\,^2\Pi)$ product was formed vibrationally much 'colder' (peak in $v=0$), but rotationally 'hot' at the higher collisional energies attained by free ablation. At the lower collisional energies achieved in the seeded mode, the $NO(X\,^2\Pi)$ displayed an even 'colder' internal state distribution, indicating that little energy flow occurs between the 'old' NO bond and 'new' CN bond. The dependence of the $NO(X\,^2\Pi)$ product state distributions on the relative translational energy of the reactants suggests that reaction (3) is governed by a predominantly direct mechanism and that the depth of any well that may exist in the potential energy surface (PES) leading to products in this channel is small compared to the total energy released by the reaction. Therefore the 'old' NO bond behaves largely as a spectator in the reaction, especially at the lower collisional energies.

2. Experimental

A schematic of the ablation apparatus is shown in Fig. 1. The two reactant beams are crossed at right angles in an octagonal reaction chamber pumped by a 2400 ℓ/s diffusion pump. Each of the two source chambers, for N_2O and C, may be differentially pumped with speeds of 2400 and 1200 ℓ/s respec-

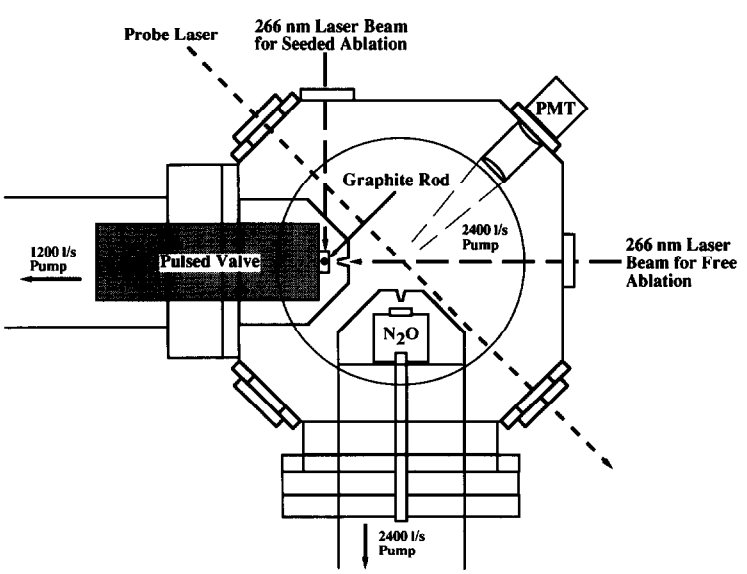

Fig. 1. An overview of the experimental apparatus allowing for collimation of both molecular beams.

tively. However, for the data reported here, only the latter is differentially pumped through a 3 mm skimmer. The pressure in the scattering chamber is maintained at $<4\times10^{-5}$ Torr with the pulsed nozzles operating at 10 Hz. The neutral beam is generated using neat N_2O (Matheson Industries, 99.99%) through a pulsed valve (Lasertechnics LPV-1, 150 μs duration, 0.5 mm diameter orifice). The stagnation pressures are identified in the figure captions for each of the spectra reported. It was verified that clustering in the neutral beam does not affect the results by repeating the spectra with a 10% N_2O/He mixture at similar stagnation pressures as the neat N_2O. Typically, the N_2O nozzle orifice is set 28–30 mm from the center of the reaction chamber. A series of scans taken at varying stagnation pressures and nozzle distances has confirmed that relaxation in the product distributions is minimal.

The carbon beam is produced by laser ablation of graphite [6]. The apparatus is designed to operate in two separate modes, one allowing the ablated material to freely expand into the reaction chamber (free ablation), while the other entrains the ablated material in a carrier gas allowing kinetic energy control of the reactant atom beam (seeded ablation). The seeded beam is generated by expanding the carrier gas through a magnetic induction-type pulsed valve (R.M. Jordan Co., 50 μs pulse, 1.0 mm diameter orifice). The effluent from the nozzle passes through the ablation region where the ablated carbon species are entrained in the jet and carried to the reaction chamber through the skimmer. He or H_2 at a stagnation pressure of 7.5 atm are used as carrier gases. For the ablation process, the fourth harmonic (266 nm) of a Nd:YAG laser (Spectra-Physics GCR-11-3, 7 ns pulse) is used. In majority of the experiments, a $\approx$3.5 mJ/pulse is focused to a spot size of $\approx$0.5 mm with a 50 cm lens onto a spectroscopic grade graphite electrode rod placed 7–9 cm from the reaction center. The rod is maintained in constant helical motion to ensure good shot-to-shot stability, and the uniform energy profile of the Nd:YAG laser beam leads to an efficient production of predominantly monomeric carbon (see below). The radiation at 266 nm has proven to be a far more efficient source for producing monomeric C than the 355 nm radiation previously used [12]. In the free ablation experiments, the laser beam enters the reaction chamber through a side port opposite the skimmer, hitting the graphite rod which has its center aligned with the laser beam (Fig. 1). For operation in the seeded mode, the ablation laser beam enters the chamber through the back port (Fig. 1), hitting the rod that is recessed with respect to the skimmer. In these experiments, it is particularly important to use a pulsed valve with a short opening time for the carrier gas, in order to minimize clustering of the carbon atoms. Typically, the ablation laser is fired 50–100 μs after triggering the Jordan valve, while the Lasertechnics valve is triggered 0–150 μs after the Jordan valve, and the probe laser is fired 25–50 μs after the ablation laser. In the free ablation mode, the probe laser is fired 15–24 μs after the ablation pulse.

A transient digitizer and a computer control data acquisition. Analog signals from the photomultiplier tubes (PMTs) are sent to a Nicolet Explorer III digital storage oscilloscope, and then to the computer for storage and processing. The timing sequence of the experiments is controlled by an array of pulse and delay generators allowing control of 6 channels with a 10 ns incremental time adjustment.

$C(^3P)$ was detected via LIF using a Nd:YAG laser pumped dye laser system (Quanta Ray, DCR1A, Quanta Ray PDL1). The dye laser, operating on rhodamine 6G, generated a beam (1.0–3.7 mJ) that was frequency doubled in a KDP crystal and focused using a 30 cm lens into the center of the freely expanding collimated effluent from the ablation. The LIF signal was normalized to laser energy on a shot-to-shot basis. Excitation of atomic carbon was achieved by a two-photon absorption at $\approx$280 nm (Fig. 2a), while fluorescence was observed at 166 nm. The fluorescence from $C(^3P)$ was imaged through a MgF window and focused with a 25 cm focal length CaF lens onto the PMT (CsI, Hamamatsu R1259). The telescope and PMT housing were first evacuated and then continually purged with Ar or N_2 when recording spectra to avoid attenuation of the VUV fluorescence.

For the detection of $NO(X\,^2\Pi)$ and $CN(X\,^2\Sigma^+)$, an excimer-laser pumped dye-laser system (Questek 2220M, Lambda Physik FL2001), operating on either QUI or coumarin 450 dyes, was used. CN was interrogated by excitation of the $\Delta v=0$, and -2 sequences of the $B\,^2\Sigma^+\leftarrow X\,^2\Sigma^+$ system [13], while NO was detected using the $\Delta v=0$ sequence of the

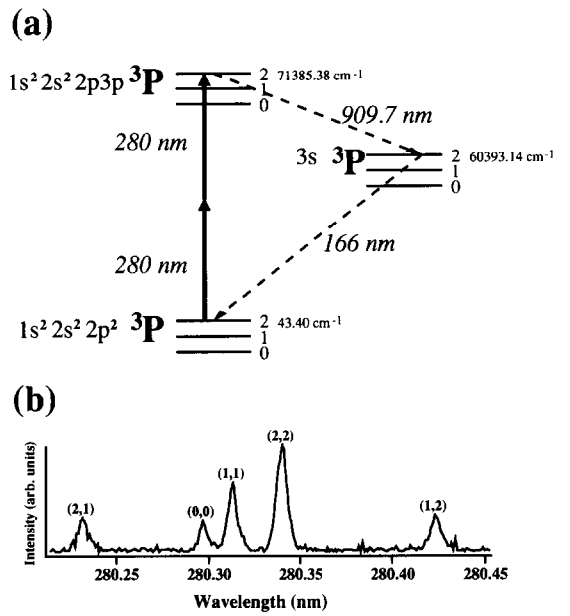

Fig. 2. (a) Detection scheme for two-photon laser excitation of ground state atomic carbon using the 2p3p $^3P_{J'} \leftarrow 2p^2\ ^3P_{J''}$ transition. The LIF is detected in the VUV near 166 nm. (b) Two-photon LIF spectrum of C(^{3}P) from 355 nm ablation of a spectroscopic grade graphite rod. Approximately 8 mJ/pulse of 355 nm was focused with a 50 cm focal length fused silica lens to a 0.4 mm spot in front of the rod. The probe laser was fired 7 μs after the ablation.

($A\,^2\Sigma^+ \leftarrow X\,^2\Pi$) system [14]. For NO, the dye laser output was frequency doubled in a BBO crystal. Typical probe energies were 20–30 μJ and 500 μJ for NO and CN respectively, focused to a spot size of ≈ 3 mm. The fluorescence from the excited molecules was imaged using a Galileo type telescope through appropriate filters and apertures onto one of two PMTs: a GaAs Hamamatsu R943-02 for CN and a solar blind CsTe Hamamatsu R166UH for NO.

3. Results and discussion

3.1. Characterization of the carbon beam

The ablation of graphite generates a variety of C_n species whose relative concentrations depend on the experimental conditions. Indeed, it has been postulated that monomeric carbon can be produced as the major species under experimental conditions in which the ablation laser dissociates the majority of the C_n species [15]. Although C(^{3}P) has been directly observed from graphite ablation [16], it was important to establish that under our experimental conditions atomic carbon is efficiently produced while the concentrations of C_3 and C_2 species are minimized.

Fig. 2 shows the C(^{3}P) LIF spectrum obtained by using two-photon absorption of focused 280 nm radiation to access the 2p3p $^3P_{J'} \leftarrow 2p^2\ ^3P_{J''}$ transition [17]. In order to achieve a high number density of carbon atoms in the detection region the apparatus was operated in the free ablation mode, probing the atomic plume 6–7 μs after the ablation pulse. Similar measurements in the seeded mode were not attempted because of the larger fluctuations in signal intensities (see below). The lines in the spectrum were identified by using published frequencies [18]. In addition, both C_2 ($D\,^1\Sigma_u^+ - X\,^1\Sigma_g^+$) [19] and C_3 ($A\,^1\Pi_u - X\,^1\Sigma_g^+$) [20] are readily detectable by LIF. This ability to directly probe C(^{3}P), C_2, and C_3 allows optimization of the experimental conditions to produce predominantly monomeric carbon, and indeed the ablation conditions given in section 2 were chosen to maximize atomic carbon and minimize the C_2, and C_3 signals.

The velocities of the C_n species obtained in the beam in the free ablation and the seeded modes were estimated by measuring LIF signals for various time delays between the ablation and the probe pulses at a fixed distance (6.5 cm). This TOF method allows measuring of not only the most probable velocity, but also the C_n velocity distribution. In these studies, LIF of C_2 rather than atomic C was detected, primarily because of the smaller shot-to-shot fluctuations in the signal when monitoring C_2. Here it is assumed that the velocity of C_2 is similar to that of C. For the seeded ablation, this assumption is validated by the fact that Naulin et al., who produced C_2 by the same method, reported a rotational temperature of the order of 10 K [21]. This would imply that sufficient collisions have taken place between C_2 and He for the former to attain the same velocity as the carrier gas. The free ablation case may be more ambiguous as not very much is understood about the ablation process itself. However, the beam formed by free ablation is directional and 'expansion-like' [22,23], which suggests that the different species may move at comparable velocities. This assumption is also supported by the observation of a maximum in the product CN and

NO signals within a microsecond of the peak of the C_2 signal.

Fig. 3a displays a velocity distribution obtained in free ablation using an ablation pulse energy of 3 mJ. It shows that the most probable velocity for the C_2 beam is ≈ 9500 m s^{-1} with a broad distribution between 7000 and 12000 m s^{-1} (at half maximum). The distributions were similar with ablation energies of 1–8 mJ/pulse. Correspondingly, for C_2 seeded in He (Fig. 3b), the most probable velocity was 1600 m s^{-1}, with a much narrower distribution centered between 1450 and 1750 m s^{-1} (at half maximum). The velocity of the N_2O beam was measured with a fast ionization gauge by recording the difference in the arrival time of the gas pulse at two different nozzle–gauge distances. At a stagnation pressure of 0.7 atm, the mean velocity of the N_2O beam was 680 m s^{-1} ($\pm 2\%$). It was not possible to accurately measure the velocity distribution of the beam using this method. Table 1 displays the velocities in each of the beams, the relative velocities and the center of mass (c.m.) collision energies. The c.m. collision energy for seeded ablation in He ranged from 0.13 to 0.17 eV, while for free ablation, the distribution ranged between 2.0 and 7.0 eV. High kinetic energies from the free laser ablation have been obtained before in other cases; for example, the energy of Al atoms obtained from the ablation of Al_2O_3 was measured to be ≈ 4 eV [24]. The large difference in the velocities (and hence collision energies) of the two modes of producing C seems to have a significant effect on the internal state distribution of the NO product as reported below. It should also be noted that in our previous report, the C velocity distribution from free ablation was *assumed* to be 3000–5000 m s^{-1} based on the C_2 TOF measurements of Dreyfus and co-workers [22,23], thus yielding a collisional energy of 0.9 ± 0.4 eV. This discrepancy may be explained by the fact that we have used much greater ablation energy (≈ 1.5 J cm^{-2}) as compared to Dreyfus et al. (0.1–0.5 J cm^{-2}). These authors have noted that the velocity of the beam increases with the ablation energy up to a certain level, above which it remains fairly constant.

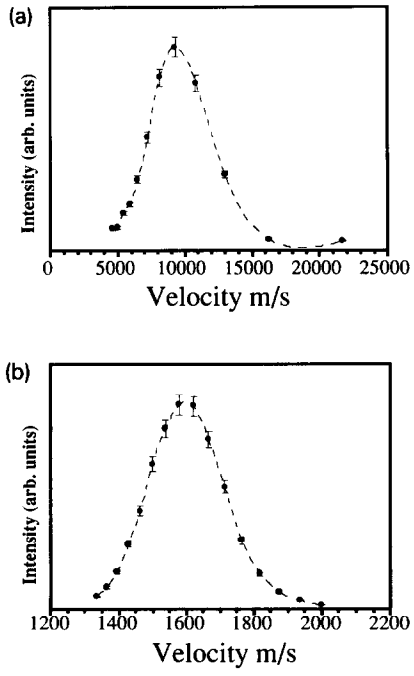

Fig. 3. Velocity distribution estimated for the C atom beam from TOF spectra of C_2 detected by LIF in the (a) free ablation mode, and (b) seeded ablation mode.

3.2. $CN(X\,^2\Sigma^+)$ and $NO(X\,^2\Pi)$ internal state distributions

A typical $CN(B\,^2\Sigma^+ \leftarrow X\,^2\Sigma^+)$ LIF spectrum obtained by using the seeded ablation mode and showing the $\Delta v = -2$ sequence is displayed in Fig. 4a. The CN product is rotationally and vibrationally 'hot' with bandheads of $v \leqslant 7$ clearly identified and a peak population in $v = 3$. The observed rovibrational excitation is in good agreement with the work of Costes et al. [12] who, using the $\Delta v = -1$ sequence, reported rotational temperatures up to 11000 K and a similar vibrational distribution. In our study, the LIF spectrum for CN did not change substantially as a function of collision energy, i.e. when producing C by free ablation (ablation energy of 15–20 mJ at 355 nm, or 3–8 mJ at 266 nm), or ablation followed by seeding in He and H_2.

Also recorded were the $NO(X\,^2\Pi)$ LIF spectra, an example of which is shown in Fig. 4b. The spectra were converted to populations by taking into account the appropriate Hönl–London line-strength factors calculated using the formulae of Earls [25], as described before [1]. In contrast to the $CN(X\,^2\Sigma^+)$ product, the NO internal state distribution was different for the low and high collisional energy regimes. Previously, we had reported for a free ablation mode

Table 1
The relative velocities and collisional energies for the free and seeded ablation methods

	C-beam velocity [a] (m/s)	N_2O-beam velocity [b] (m/s)	Relative velocity (m/s)	Collisional energy [c] (eV)
free ablation	9500±2500	680	9525±2500	4.5±2.5
seeded ablation (He)	1600±150		1740±150	0.15±0.02

[a] The width of the velocity distribution is taken at half maximum.
[b] Peak of the velocity distribution.
[c] Center of mass collisional energy.

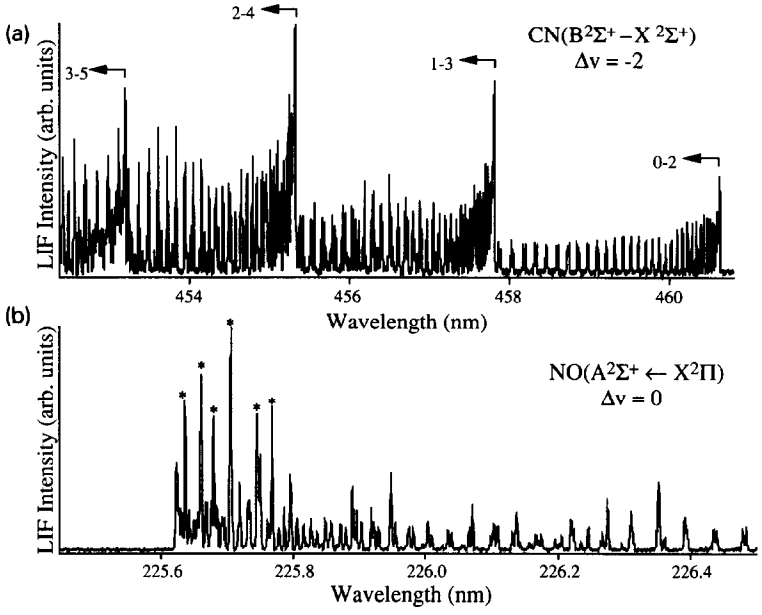

Fig. 4. Product LIF spectra observed from the title reaction using seeded ablation. (a) CN($B\,^2\Sigma^+ \leftarrow X\,^2\Sigma^+$) LIF spectrum. The $\Delta v = -2$ sequence was excited and fluorescence observed on the $\Delta v = 0$ sequence. The C(^{3}P) beam was entrained with a stagnation pressure of 7.5 atm H_2. The N_2O beam was neat with a stagnation pressure of 0.7 atm. (b) NO ($A\,^2\Sigma^+ \leftarrow X\,^2\Pi$) LIF spectrum. The $\Delta v = 0$ sequence was used for excitation and the observation of fluorescence. The C(^{3}P) beam was entrained with a stagnation pressure of 7.5 atm He. The N_2O beam was neat with a stagnation pressure of 0.7 atm. Some of the peaks that have been marked with an asterisk, likely originate from the Mulliken bands ($D\,^1\Sigma_u^+ \leftarrow X\,^1\Sigma_g^+$) of C_2.

(355 nm, pulse energy of 15–20 mJ) a high degree of rotational excitation with levels in excess of $J = 60.5$ being detected. The rotational distribution for the $v = 0$ level of NO($^2\Pi_{1/2}$) was inverted peaking in $J = 49.5$. Some population was also observed in $v = 1$ and $v = 2$ with population ratios being $v = 0:1:2 = 1:0.45:0.12$. Similar distributions were obtained for NO($^2\Pi_{3/2}$). In the free ablation mode employed for this study, the NO LIF spectra was obtained by using 266 nm ablation with a pulse energy of 3.5 mJ at delays 15–24 μs. Fig. 5a shows the corresponding rotational distribution. It appears to be bimodal with two peaks at $\approx J = 9.5$ and 25.5 and states up to $J = 40.5$ being populated. Some population in vibrational lev-

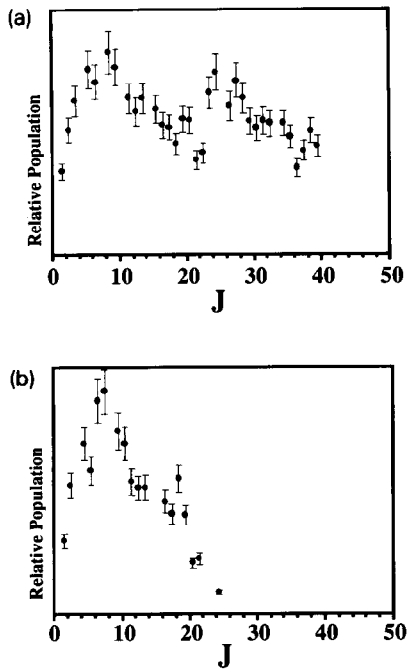

Fig. 5. Nascent rotational distributions of the $v=0$ level of NO obtained in free and seeded ablation modes, using 266 nm radiation. (a) Free ablation mode. The N_2O beam was neat with a stagnation pressure of 2.3 atm. (b) Seeded ablation mode. The $C(^3P)$ beam was entrained with a stagnation pressure of 7.5 atm He. The N_2O beam was neat with a stagnation pressure of 0.7 atm.

els up to $v=2$ was also found, although less than under the conditions reported in ref. [1]. The rotational distribution did not change when the stagnation pressure (and hence the background chamber pressure) was reduced, and when increasing the distance of the N_2O nozzle from the reaction center. Also, varying the delay between the ablation and probe lasers from 15 to 24 μs did not have a significant effect on the rotational distribution. Shorter time delays could not be used because of interference from a background 'glow' from the free ablation. It therefore appears that in free ablation, the experimental ablation conditions (at 355 or 266 nm) have an effect on the NO energy disposal, in particular on the rotational distribution. This observation, though difficult to fully rationalize, may be a result of changes in the C_n species velocity as a function of ablation conditions, as reported before. The bimodal nature of the distribution may not be entirely surprising considering the broad energy distribution of collision energies in the free ablation mode (Table 1). It is also possible that the velocity distribution generated in the experiments reported in ref. [1] by using 355 nm ablation at high pulse energies (which was not measured) is different than that from the 266 nm ablation used in this work. However, it is quite clear that free ablation in general does not provide a narrow energy distribution, thereby complicating interpretations. In particular, since the products were detected at relatively long delays they may reflect preferentially reactions at the lower end of the collision energy distribution. At 15–24 μs delays, products are detected that are either formed inside the probe region in reactions of slower moving carbon atoms, or formed in reactions of faster carbon atoms outside the probe region, and scattered into it. The latter may be partially relaxed, but based on considerations of scattering angles and detection efficiency, they will be detected less efficiently than products formed inside the probe volume.

The $NO(v=0)$ rotational distribution obtained in the seeded ablation (Fig. 5b) was substantially colder, peaking around $J=8.5$. Also, no population was observed in $v>0$. These results were similar when seeding in either He or H_2 and changing the delay between the ablation and probe lasers from 25 to 50 μs. It must be emphasized that in the data analysis, populations obtained from several scans over the same spectral region were averaged. This was necessary because there are momentary fluctuations in the plasma producing the atomic carbon. These fluctuations, in turn, lead to momentary changes in the C-beam intensity, randomly enhancing or diminishing certain peaks by as much as 30%. However, the *shape* of the distribution curve was similar in each of the scans.

An examination of the NO LIF spectrum reveals a number of features not assignable to the $NO(A\,^2\Sigma^+ \leftarrow X\,^2\Pi)$ transition, which are much weaker in the free ablation as compared to the seeded mode. These peaks likely originate from the Mulliken bands ($D\,^1\Sigma_u^+ \leftarrow X\,^1\Sigma_g^+$) of C_2 [21] and some of them have been marked with an asterisk in Fig. 4b. By performing scans with only the ablation source operating, signals were observed in the (0, 0) and (1, 0) bandhead regions which are definitely assignable to the C_2 Mulliken bands. However, since the overlap is observed only with a small region of the $NO(A\,^2\Sigma^+ \leftarrow X\,^2\Pi)$ (0, 0) band, they do not consti-

tute a major problem in the data analysis. Also, C_3 LIF signals have been observed in the seeded ablation work due to the Swing bands ($A\,^1\Pi_u \leftarrow X\,^1\Sigma_g^+$) which have a strong absorption in the region of the $CN(B\,^2\Sigma^+ \leftarrow X\,^2\Sigma^+)$ $\Delta v=0$ sequence. However, neither C_2 and C_3 nor higher order clusters will participate in exoergic reactions with N_2O. The removal rate coefficients of C_2 and C_3 by N_2O are $\leqslant 10^{-14}$ cm^3 molecule^{-1} s^{-1} [26].

It is important to realize that the quantity measured by LIF is a number density, i.e. the total number of molecules in a specific quantum state within the irradiated volume. To determine the exact population for a given quantum state, a number density-to-flux transformation (DFT) is required [27]. The need for the DFT arises due to the fact that reaction products created in different internal energy states will expand in space at different velocities. However, for this report, no attempt was made to correct for density-to-flux effects. For an effective DFT, both reactant beams need to be collimated, which necessitated higher signal levels than were obtained in this study. However, even without this correction, the $CN(B\,^2\Sigma^+ \leftarrow X\,^2\Sigma^+)$ LIF spectra obtained in the present work are in good qualitative agreement with those obtained by Costes et al. under conditions where density-to-flux corrections could be applied. The authors found the DFT corrections were small even for highly excited $CN(X\,^2\Sigma^+)$ fragments [11,12]. Hence, it is expected that corrections for the density-to-flux effects will not change the qualitative conclusions of this work.

3.3. Implications to the reaction dynamics

The dynamics for reactive processes are usually divided into two categories: direct and indirect [28]. Put in simple terms, direct reactions are described by a stripping dynamics and characteristically one of the reaction products is born with considerably more internal energy than the other. For these reactions, the well depth along the reaction coordinate is too shallow to allow energy randomization among the products to occur. Product state distributions from a direct reaction are usually nonstatistical with a significant fraction of the available energy, E_{avail}, channeled into product translation. In addition, a far greater amount of E_{avail} is channeled into the newly formed bond, as opposed to the 'old' bond. In contrast, an indirect reaction proceeds through a bound transition state whose lifetime may be sufficiently long for energy randomization among the products to occur. In this case, the products internal energy state distributions are often statistical. In the title reaction, theoretical calculations propose a potential well along the reaction coordinate and formation of a CNNO reactive intermediate [4,5]. If this intermediate survives for several vibrational periods, energy could flow from the new CN bond into the old NO bond. Thus an increase in the internal state excitation for the NO products upon *decreasing* the kinetic energy of the reactants may occur. However, our preliminary findings indicate that this is not the case. Instead, the internal energy in both the vibrational and rotational degrees of freedom of $NO(X\,^2\Pi)$ increases at higher kinetic energies. This points towards a reaction that is predominantly governed by a direct or stripping type mechanism. The high level of internal excitation in the $CN(X\,^2\Sigma^+)$ product at all kinetic energies investigated is consistent with an attractive potential where energy is released as the reactant C atoms approach the terminal nitrogen end of the linear N_2O molecule [4,5].

The higher level of internal excitation in the $NO(X\,^2\Pi)$ product at higher collision energies may be rationalized by two possible mechanisms: the reaction is highly exoergic with an intermediate complex, or alternatively, it is truly direct where even if an intermediate is formed, it is short lived. In the first case, at the higher collisional energies employed, it is likely that a larger number of reactive trajectories with a greater range of impact parameters becomes accessible. Thus, the reaction may proceed through intermediate complexes that are bent either in the cis or trans configuration [4,5]. Indeed, the broad range of velocities shown in Fig. 3a, could reflect a wide range of impact parameters. When these bent intermediates fall apart into products, a torque is imparted on the reaction products manifesting itself as rotational excitation. Trajectories in which the approach is end on (zero impact parameter) may also transfer more energy into the NO bond through impulsive energy release. Increasing the collision energy will thus produce more vibrational excitation in $NO(X\,^2\Pi)$. A similar observation, i.e. conversion of higher collisional energy into product internal energy has been

made for the reaction $Si+N_2O$ [29]. This reaction is endoergic, and was found to have a threshold of about 0.3 eV. At energy values above the threshold, the rotational excitation of the product $SiN(X\,^2\Sigma^+)$ was directly proportional to the excess collisional energy. However, in our study, the relatively small internal excitation at the lower collisional energies for NO would suggest a direct mechanism, where an intermediate, if formed, is short-lived. Indeed, a long-lived intermediate is not expected in an exothermic reaction such as the title reaction. In this regard, a comparison with a theoretical study [30] of the reaction $C(^3P)+NO$ using a quasi-classical trajectory treatment, may be useful. In that study, the rotational excitation of the product $CN(X\,^2\Sigma^+)$ was linked to the orbital angular momentum, which in turn is proportional to the relative velocity of the reactants. Therefore, a higher relative velocity (and thus collisional energy) is observed as higher rotational excitation of the product.

Classical trajectory calculations on the title reaction were run on a PES constructed using a MNDO semi-empirical CI SCF calculation [4,5]. The calculations were restricted by the assumption that the CNNO intermediate behaves as a pseudo-triatomic CNN′ intermediate; i.e. the NO bond was frozen in the calculations to reduce the dimensionality of the problem and reduce the computational time required. The theoretical surface used for the trajectory calculations was a triplet of A″ symmetry and possessed a well favoring the formation of a collision complex. These calculations predicted an inverted vibrational energy distribution for the CN product peaking at $v=10$–12. Although the excitation is considerably higher than the experimentally observed peak at $v=3$, the excitation of higher vibrational levels is qualitatively consistent with the mechanism suggested by the calculations. The vibrational population inversion, despite the presence of a well, was attributed to the high exoergicity of the reaction, and it was concluded that the reaction possesses some direct character. It has been shown that for surfaces with deep wells, the intermediate lifetime will fall dramatically at high collision energies with the interaction tending towards direct. However, a more detailed theoretical study providing for energy flow into the NO bond should provide more insight into the dynamics of this reaction.

In conclusion, it appears from our studies that the reaction channel leading to $CN(X\,^2\Sigma^+)$ and $NO(X\,^2\Pi)$ proceeds through a reaction mechanism that is predominantly direct, where the NO behaves as a spectator. Additional experiments at a lower collisional energy may be necessary to determine if this reaction does posses some indirect character, and if the collisional complex may live longer. This in turn, could lead to more internal excitation of the NO product.

Acknowledgement

The authors would like to thank Scott A. Reid and Michel Costes for invaluable advice and assistance during the design phase and initial evaluation of the results of this work. DCS and MRS are grateful to the US Department of Education for graduate fellowships. The research was supported by the US Department of Energy, Office of Energy Research, Division of Chemical Sciences.

References

[1] S.A. Reid, F. Winterbottom, D.C. Scott, J. de Juan and H. Reisler, Chem. Phys. Letters 189 (1992) 430.
[2] M. Costes, G. Dorthe and M. Destriau, Chem. Phys. Letters 61 (1979) 588.
[3] H. Sekiya, M. Tsuji and Y. Nishimura, J. Chem. Phys. 84 (1986) 3739.
[4] R. Bouachir, M.T. Rayez, B. Duguay and J.C. Rayez, Chem. Phys. 90 (1984) 325.
[5] J.C. Rayez, M.T. Rayez and B. Duguay, J. Chem. Phys. 78 (1983) 827.
[6] M. Costes, C. Naulin, G. Dorthe, G. Daleau, J. Joussot-Dubien, C. Lalaude, M. Vinckert, A. Destor, C. Vaucamps and G. Nouchi, J. Phys. E 22 (1989) 1017.
[7] I.P. Herman, Chem. Rev. 89 (1989) 1323.
[8] C.E.M. Strauss, S.H. Kable, G.K. Chawla, P.L. Houston and I.R. Burak, J. Chem. Phys. 94 (1991) 1837.
[9] H.F. Krause, Chem. Phys. Letters 81 (1981) 78.
[10] W.R. Gentry and C.F. Giese, Rev. Sci. Instr. 49 (1979) 595.
[11] C. Naulin, M. Costes and G. Dorthe, Chem. Phys. 153 (1991) 519.
[12] M. Costes, C. Naulin, G. Dorthe and Z. Moudden, Laser Chem. 10 (1990) 367.
[13] L.L. Danylewych and R.W. Nicholls, Proc. Roy. Soc. A. 360 (1978) 557.
[14] I. Deezsi, Acta Phys. 61 (1958) 125.
[15] M.M. Stevanovic, Intern. J. Thermophys. 4 (1983) 127.

[16] H. Bergström, H. Hallstadius, H. Lundberg and A. Persson, Chem. Phys. Letters 155 (1989) 27.
[17] P. Das, G. Ondrey, N. van Veen and R. Bersohn, J. Chem. Phys. 79 (1983) 724.
[18] C.E. Moore, Atomic energy levels, NSRDS-NBS Circular No. 467, a6 I-1 (US GPO, Washington, 1970).
[19] O.G. Landdsverk, Phys. Rev. 56 (1939) 769.
[20] G. Herzberg, Spectra of polyatomic molecules (Van Nosrtand Rheinhold, New York, 1950).
[21] C. Naulin, M. Costes and G. Dorthe, Chem. Phys. Letters 143 (1988) 496.
[22] R.W. Dreyfus, R. Kelly, R.E. Walkup and R. Srinivasan, SPIE Vol. 710, Excimer Laser Opt. 17 (1986) 46.
[23] R.W. Dreyfus, R. Kelly and R.E. Walkup, Nucl. Instr. Methods B 23 (1987) 557.
[24] R.W. Dreyfus, R. Kelly and R.E. Walkup, Appl. Phys. Letters 49 (1986) 1478.
[25] L.T. Earls, Phys. Rev. 48 (1935) 423.
[26] H. Reisler, M. Mangir and C. Wittig, unpublished results.
[27] D.M. Sonnenfroh and K. Liu, Chem. Phys. Letters 176 (1991) 183.
[28] J.C. Polanyi, Accounts Chem. Res. 5 (1972) 161.
[29] C. Naulin, M. Costes, Z. Moudden, N. Ghanem and G. Dorthe, Chem. Phys. Letters 202 (1993) 452.
[30] P. Halvick and J.C. Rayez, Chem. Phys. 131 (1989) 375.